Synthesis and Properties of New Photosensitive Triazene Polyacrylates

EMIL C. BURUIANA,[1] TINCA BURUIANA,[1] HAHUI LENUTA,[1] THOMAS LIPPERT,[2] LUKAS URECH,[2] A. WOKAUN[2]

[1]Petru Poni Institute of Macromolecular Chemistry, Romanian Academy, 41 A Grigore Ghica Voda Alley, 700487, Iasi, Romania

[2]Paul Scherrer Institut, 5232 Villigen PSI, Switzerland

Received 25 April 2006; accepted 23 June 2006
DOI: 10.1002/pola.21653
Published online in Wiley InterScience (www.interscience.wiley.com).

ABSTRACT: 1-(Phenyl)-3-(2-acryloyloxyethyl)-3-methyl triazene-1 (M1) and 1-(*p*-nitrophenyl)-3-(2-acryloyloxyethyl)-3-methyl triazene-1 (M2) were synthesized to study the substituent effect of the triazene unit on the copolymerization with methyl methacrylate (MMA). From the ^{1}H NMR spectra of the resulting copolymers, their compositions were determined to be 1:3.18 M1/MMA and 1:2.45 M2/MMA, respectively. The polymers were examined with respect to their structure, thermal properties, and surface morphology. The influence of the triazene structure on the photosensitive properties of the copolymers exposed to ultraviolet/laser irradiation was also investigated and compared with that of the parent derivatives. The copolymer containing the phenyl triazene chromophore as the photochemically most active group exhibited a low threshold of ablation and a high etching rate for fluences under 400 mJ cm^{-2}. Scanning electron microscopy images confirm the formation of ablated craters more clearly in the copolymer made with M1, for which the thermal effects of the ablation mechanism were visible only with 2500× magnification. © 2006 Wiley Periodicals, Inc. J Polym Sci Part A: Polym Chem 44: 5271–5282, 2006

Keywords: acrylates; atomic force microscopy; NMR; photochemistry; polyacrylates; triazene; UV/laser ablation

INTRODUCTION

Polymers containing photosensitive moieties have attracted great interest because of their potential use in various applications, the foremost of these including devices for optical data storage,[1] photoresists,[2] and photolithographic assemblies.[3] Moreover, the design and synthesis of polymers highly sensitive to light processing continue to be the most attractive targets because various material properties can be improved by the incorporation of appropriate chemical structures into a polymer backbone. An interesting topic in this field is the fabrication of artificial surface relief structures in films based on triazene polymers upon their exposure to ultraviolet (UV)/laser irradiation, which are particularly exploitable as dry etching resists in microlithography.[4–7] These materials are usually characterized by the presence of triazene chromophores able to undergo facile photochemical cleavage with the release of molecular nitrogen during the laser–solid interaction.[8–10]

In the context of the notable progress made in understanding polymer ablation[11] with direct consequences for the structuring of surfaces, the triazene polymers are considered materials of

Correspondence to: E. C. Buruiana (E-mail: emilbur@icmpp.ro)

great promise for excimer laser ablation lithography[12] as a complementary technique to conventional photolithography. Viewed from this perspective, some polymers with triazene functions (Ph—*N*=*N*—*N*—), such as polyesters, polyethers, poly(methyl methacrylate)s (PMMAs), polysulfones, and polytriazenes, have been tested with UV/laser ablation.[13–17] Comparisons of their microstructural characteristics with those of commercial polymers (i.e., polyimide and PMMA) have been made. Above all, it has already been argued that the triazene polymers reveal superior ablation properties for irradiation wavelengths at about 308 nm.[18] For this reason, the investigation of such designed photopolymers represents a target opportunity to develop and characterize novel systems into interdisciplinary research.

Our group has also been active in this area, studying triazene polyurethanes based on new monomers[19–22] by changing the substituent attached to the triazene group and the concentration and position of the chromophores inserted into the polymer backbone with a significant effect on the polymer properties. In this article, we describe the synthesis of triazene acrylate and the corresponding copolymers with methyl methacrylate (MMA). After confirming the structures of the resultant copolymers, we investigate properties such as the thermal stability and surface morphology of films cast from solutions together with the photochemical response under UV/laser irradiation. We now report the results of the first study of triazene polyacrylates as a continuation of our effort to develop novel photoionomers bearing stilbene,[23,24] pyrene,[25] anil,[26] and azobenzene chromophores,[27–30] whose thin films have excellent fluorescent, photochromic, or photodegradable properties.

EXPERIMENTAL

Monomer Synthesis

A stirred solution of aniline (10 g, 0.107 mol) in HCl 12% (70 mL) was cooled to 0 °C and diazotized with an aqueous solution of sodium nitrite (7.4 g, 0.107 mol). The reaction mixture was added dropwise to a solution of 8 g of *N*-methyl ethanol amine (0.107 mol) and 28.4 g (0.268 mol) of sodium carbonate in 50 mL of water at 0 °C over 1 h. Then, 5 g of sodium chloride was added, and the resulting mixture was extracted twice with Et_2O. The organic layer was dried (Na_2SO_4) and concentrated under reduced pressure, resulting in 1-(phenyl)-3-(2-hydroxyethyl)-3-methyl triazene-1 (P1) as a brown, viscous oil.

Yield: 12.53 g (70%). ELEM. ANAL. Calcd. for $C_9H_{13}N_3O$: C, 60.33%; H, 7.26%; N, 23.46%. Found: C, 60.30%; H, 7.24%; N, 23.44%. ^{1}H NMR [dimethyl sulfoxide-d_6 (DMSO-d_6), δ, ppm]: 7.43 (d, 2H, ortho aromatic protons to triazene), 7.35 (t, 2H, meta aromatic protons to triazene), 7.17 (t, 1H, para aromatic proton to triazene), 3.81 (s, 4H, CH_2CH_2OH), 3.28 (s, 3H, CH_3—N—N=N). IR (KBr, cm^{-1}): 3350 (OH), 2920 (CH), 1595 (aromatic CH), 1350 (N=N—N), 750, 690 (monosubstituted aromatic ring).

1-(Phenyl)-3-(2-acryloyloxyethyl)-3-methyl triazene-1 (M1) was synthesized through the reaction of 0.05 mol (9.5 g) of the triazene precursor (P1) with 0.05 mol (4.8 mL) of acryloyl chloride in methylene chloride and in the presence of triethyl amine (7 mL, 0.05 mol) at 0–5 °C. The reaction mixture, maintained at room temperature with stirring for 3 days, was filtered, extracted, and washed several times with water and was then dried over Na_2SO_4. The triazene acrylic monomer (M1) was collected after the removal of the solvent.

Yield ($C_{12}H_{15}N_3O_2$): 7.4 g (82%). ^{1}H NMR (DMSO-d_6, δ, ppm): 7.45 (d, 2H, ortho aromatic protons to triazene), 7.33 (t, 2H, meta aromatic protons to triazene), 7.14 (t, 1H, para aromatic protons to triazene), 6.38 (d, 1H, trans olefinic proton CH_2), 6.09 (m, 1H, olefinic proton CH), 5.78 (d, 1H, cis olefinic proton CH_2), 4.38 (t, 2H, CH_2CH_2OCO), 3.98 (t, 2H, CH_2CH_2OCO), 3.25 (s, 3H, CH_3—N—N=N). IR (KBr cm^{-1}), 1720 (CO), 1630 (CH=CH), 1350 (N=N—N), 690, 760 cm^{-1} (monosubstituted aromatic ring).

Similarly, with *para*-nitroaniline under the aforementioned conditions, the 1-(*para*-nitrophenyl)-3-(2-hydroxyethyl)-3-methyl triazene-1 (P2) precursor (yellow crystals) was prepared to obtain 1-(*p*-nitrophenyl)-3-(2 acryloyloxyethyl)-3-methyl triazene-1 (M2) as brown crystals.

P2

Yield ($C_9H_{12}N_4O_3$): 18.06 g (75%). ELEM. ANAL. Calcd.: C, 48.21%; H, 5.35%; N, 25.0%. Found: C, 48.19%; H, 5.33%; N, 24.95%. ^{1}H NMR (DMSO-d_6, δ, ppm): 8.11 (d, 2H, meta aromatic protons to triazene), 7.42 (d, 2H, ortho aromatic protons to triazene), 3.94 (s, 4H, CH_2CH_2OH), 3.64 (s, 1H, OH), 3.3 (s, 3H, CH_3—N—N=N). IR (KBr, cm^{-1}): 3500 (OH), 2950 (CH_2), 1595 (aromatic ring),

1510 (NO_2), 1350 (N=N—N), 860 (disubstituted aromatic ring).

M2

Yield ($C_{12}H_{14}N_44O_4$): 11.8 g (85%). ^{1}H NMR (DMSO-d_6, δ, ppm): 8.16 (d, 2H, meta protons to triazene), 7.46 (d, 2H, ortho aromatic protons to triazene), 6.4 (d, 1H, trans olefinic proton CH_2), 6.1 (m, 1H, olefinic proton CH), 5.83 (d, 1H, cis olefinic proton CH_2) 4.45 (t, 2H, CH_2CH_2OCO), 4.12 (t, 2H, CH_2CH_2OCO), 3.30 (s, 3H, CH_3—N—N=N). IR (KBr, cm^{-1}): 1720 (CO), 1625 (CH=CH), 1590 (aromatic ring), 1505 (NO_2), 1325 (N=N—N), 850 (disubstituted aromatic ring).

Polymer Synthesis

The preparation of copolymers of M1 or M2 with MMA was performed by free-radical polymerization with a starting comonomer ratio of 1:2.33 in a solution of dioxane (30 wt %) in sealed glass ampules at 60 °C for 3 days in the presence of 2.2′-azobisizobutyronitrile (AIBN; 0.2%) as the initiator. The resulting copolymers were precipitated in methanol and dried for 48 h under reduced pressure.

1-(Phenyl)-3-(2 acryloyloxyethyl)-3-methyl triazene-1-co-methyl methacrylate (T-PAc1)

^{1}H NMR (DMSO-d_6, δ, ppm): 7.1–7.4 (aromatic protons from M_1), 3.69–4.3 (CH_2—CH_2 from M_1), 3.58 (—$COOCH_3$ from MMA), 3.29–3.37 (N—CH_3), 1.5–2.2, (CH—$COOCH_3$), 0.8–1.5 (CH_2 from M_1; CH_2 and CH_3 from MMA).

1-(p-Nitrophenyl)-3-(2 acryloyloxyethyl)-3-methyl triazene-1-co-methyl methacrylate (T-PAc2)

^{1}H NMR (DMSO-d_6, δ, ppm): 8.13, 7.45 (aromatic protons from M_2), 3.9–4.42 (CH_2—CH_2 from M_2), 3.55 ($COOCH_3$ from M_2), 3.2–3.33 (N—CH_3), 1.4–2.1 (CH—$COOCH_3$ from MMA), 0.7–1.3 (CH_2 from M_2; CH_2 and CH_3 from MMA).

Measurements

The IR spectra were recorded on a Specord M80 spectrophotometer. The ^{1}H NMR spectra were recorded on a Bruker 400-MHz spectrophotometer with tetramethylsilane as an internal standard. The UV absorption spectra were measured with a Specord M42 spectrophotometer in solutions and thin films. The molecular weight distributions of the copolymers were determined with a PLEMD 950 apparatus equipped with two PLgel mixed columns. Thermogravimetric analyses (TGAs) were conducted in air on a MOM (Budapest) derivatograph at a heating rate of 12 °C min^{-1}. For UV spectroscopy investigations, the samples were exposed to UV irradiation with a high-pressure mercury lamp. A Digital Instrument model DI 5000 atomic force microscope was used to probe the surface morphology. The film thickness of the films was determined with an interferential microscope (Linnik). The laser ablation rate and the ablation threshold fluence (F_{th}) were obtained by the irradiation of solvent-cast polymer films with a XeCl laser (wavelength = 308 nm, pulse length (τ) = 30 ns; Compex 205, Lambda Physic). The resulting ablation craters in the polymer were measured with a Sloan Dektak 8000 profilometer (Veeco) and were plotted against the pulse number for each irradiation fluence (F). The slopes of these individual curves corresponded to the ablation rates for the corresponding fluence. The ablation rates were then plotted versus the fluence and fitted according to eq 1:[31]

$$d(F) = \frac{1}{\alpha_{eff}} \ln\left(\frac{F}{F_{th}}\right) \quad (1)$$

where $d(F)$ represents the ablation rate per pulse and α_{eff} is the effective absorption coefficient. F_{th} is defined as the minimum fluence at which the onset of ablation can be observed. For scanning electron microscopy (SEM) images, an ABT-60 scanning electron microscope (Topcon) was used.

RESULTS AND DISCUSSION

Characterization of the Triazene Acrylates and Copolymers

Two new acrylic monomers with phenyl triazene (M1) and *para*-nitrophenyl triazene units (M2) were synthesized through the esterification of P1 or P2 with acryloyl chloride, which was previously obtained by a coupling reaction of diazotized (*para*-NO_2)aniline with *N*-methyl ethanol amine in a basic medium, as shown in Scheme 1. The chemical structures of the triazene monomers (M1 and M2) and the parent precursors (P1 and P2) were confirmed with elemental analysis, IR/UV, and ^{1}H NMR spectroscopy data. The deter-

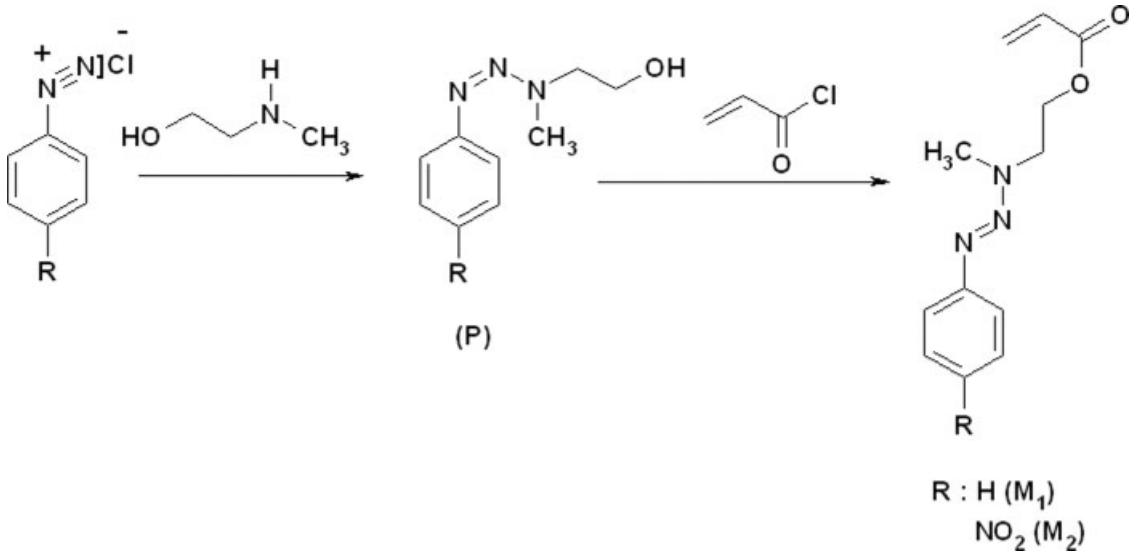

Scheme 1. Synthesis of triazene acrylate monomers (M1 and M2).

mined values of elemental analysis given in the Experimental section are very close to the theoretical ones. For exemplification, the ^{1}H NMR spectrum of M2 is shown in Figure 1, and it is in good agreement with the expected structure. In comparison with P2 (not shown here), for which the resonance of protons attributed to CH_2—CH_2 appears as singlet proton peak at 3.94 ppm, in M2 two triplets at 4.45 ppm (CH_2OCO) and at 4.12 ppm (CH_2—*N*—*N*=*N*—) can be observed as result of the esterification reaction.

The protons in the meta position (2H) adjacent to the triazene moiety can be seen at 8.17 ppm, whereas those in the ortho position are present at 7.48 ppm. The doublet peak due to the olefinic proton (CH) appears at 6.14 ppm, and the peaks assigned to CH_2 protons in a cis (multiplet) or trans (doublet) configuration have been identified at 5.81 and 6.48 ppm, respectively. Another peak at 3.32 ppm belongs to the protons from CH_3 linked to triazene. Monomer M1 has an NMR spectrum analogous to that of M2, with a differ-

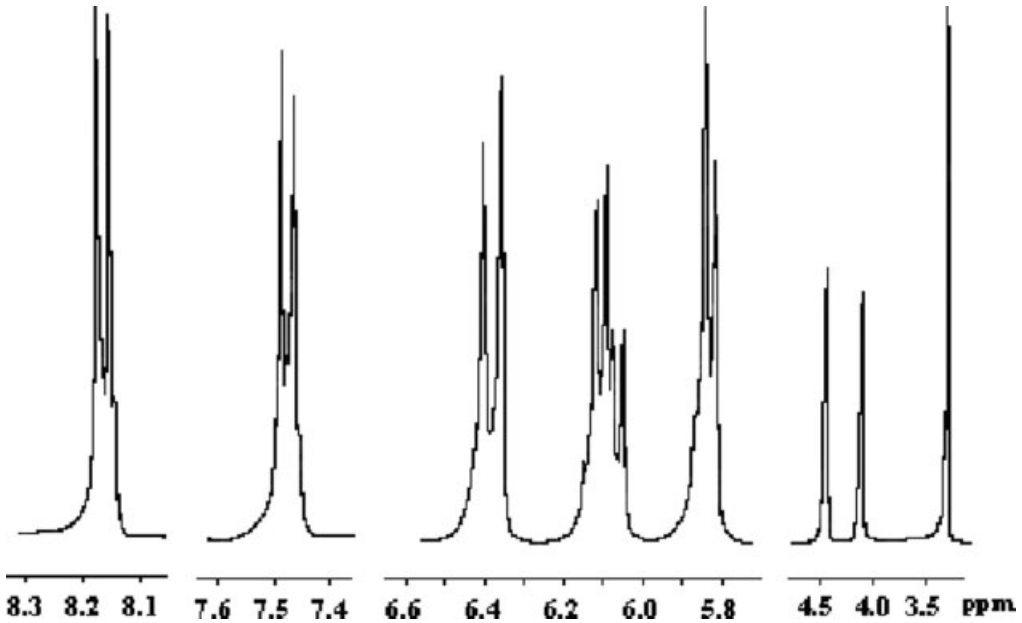

Figure 1. ^{1}H NMR spectrum of M2.

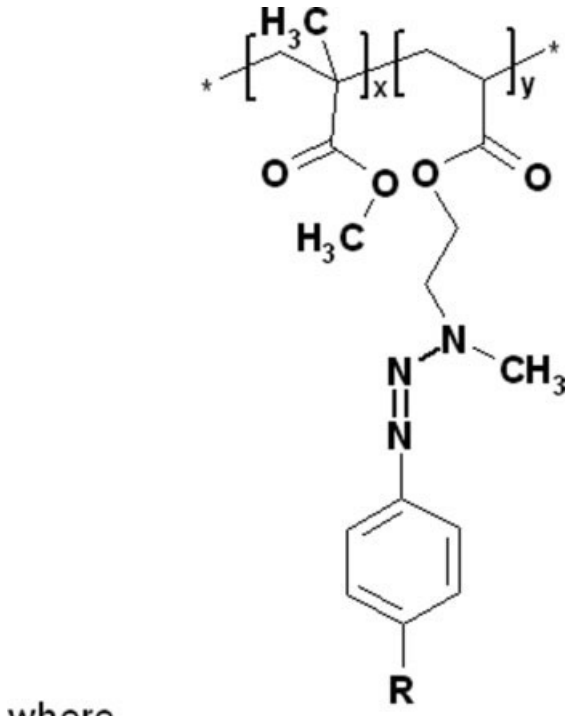

Scheme 2. Schematic representation of the triazene polyacrylate structure (T-PAc1 and T-PAc2).

ence in the aromatic zone, in which three signals of the aromatic protons appear at 7.46 (2H, d, ortho to triazene), 7.34 (2H, t, meta to triazene), and 7.15 ppm (1H, t, para to triazene). Also, the presence of aliphatic protons at a higher field at about 0.1 ppm has been evidenced. As shown in Scheme 2, the corresponding copolymers of M1 and M2 with MMA were prepared by free-radical polymerization with AIBN as the initiator (T-PAc1 and T-PAc2). Both polymers are readily soluble at room temperature in common organic solvents such as chloroform, dichloromethane, tetrahydrofuran, and dimethylformamide (DMF), and their solutions can be formed via casting onto various good-quality substrate films. The weight-average molecular weight (M_w) of T-PAc1 was 193,400 [weight-average molecular weight/number-average molecular weight (M_w/M_n) = 1.9], and, M_w was 220,600 ($M_w/M_n = 1.8$) for T-PAc2, as measured by gel permeation chromatography with respect to monodisperse polystyrene standards.

In the IR spectra, the synthesized copolymers exhibit absorption bands of the parent monomers, with the exception of the stretching vibration of the C=C double bond, which confirms the polymerization of the monomeric units. Characteristic of the triazene structure chemically anchored to the polymeric chain is the absorption at 1375 cm^{-1}.

The ^1H NMR spectrum of the T-PAc2 copolymer is presented in Figure 2. The most interesting peaks in this polymer are those assigned to the aromatic protons located at 8.13 and 7.45 ppm and the aliphatic ones from the spectral zone of 2.2–0.8 ppm because these signals can be used to calculate its composition. In fact, from the ratio of the peak integral for aliphatic protons that originated from the acrylic backbone to that of the aromatic protons in the NMR spectrum, a molar ratio of the two monomer components (M2/MMA) of 1:2.45 was found for T-PAc2. We can see that the copolymer composition determined via NMR spectroscopy by integration of the aforementioned signals does not coincide with the corresponding feed ratio because of the reactivity difference between

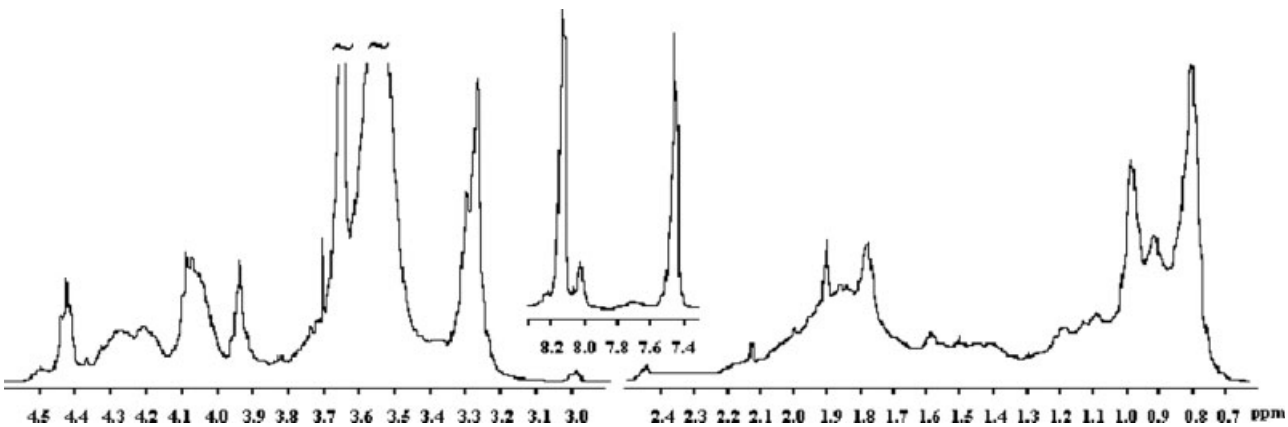

Figure 2. ^1H NMR spectrum of T-PAc2.

Table 1. Characteristics of the Triazene Acrylic Copolymers

Sample	Elemental Analysis (%)				Ultraviolet–Visible (nm)	M_w (g/mol)	M_w/M_n
		C	H	N			
T-PAc1	Calcd.	60.87	6.82	8.78	286, 322 (DMF)	193,400	1.9
	Found	60.85	6.79	8.65	284, 313 (film)		
T-PAc2	Calcd.	56.17	6.61	9.39	364 (DMF)	220,600	1.8
	Found	56.14	6.58	9.36	366 (film)		

triazene acrylate and MMA, the reactivity being slightly higher in the latter. Additionally, an unsaturated structure with minor peaks between 5.8 and 6.4 ppm, possibly generated by a disproportionation reaction, can be observed in the aforementioned spectrum. Similarly, the ratio of 1:3.18 M1/MMA, calculated for T-PAc1, is close to that found by elemental analysis from the nitrogen content (Table 1). The introduction of an electron-acceptor substituent in the triazene monomer has resulted in a modest increase in the reactivity in the copolymerization.

Because the decomposition temperature of the polymers has a pronounced influence on the ablation quality, the thermal stability of the triazene copolymers has been investigated with TGA. In the case of T-PAc1, the first thermal decomposition step occurs between 110 and 169 °C, indicating around 23% weight loss (not shown). As assumed, the main decomposition process of this polymer results from the decomposition of the triazene fragment. For T-PAc2, the first stage of the thermal process starts at 122 °C and reaches 206 °C when 25% weight loss is noticed.

To quantify some aspects of the classic picture of acrylic copolymer morphology, the surface topography of the T-PAc2 copolyacrylate on a quartz substrate has been examined with atomic force microscopy (AFM). For better visibility of the details, some different positions per substrate have been taken. Figure 3 displays the surface image of the polymeric film of T-PAc2 obtained via casting from a DMF solution. The structure of the film (thickness $\approx$ 1.68 μm) corresponds to the

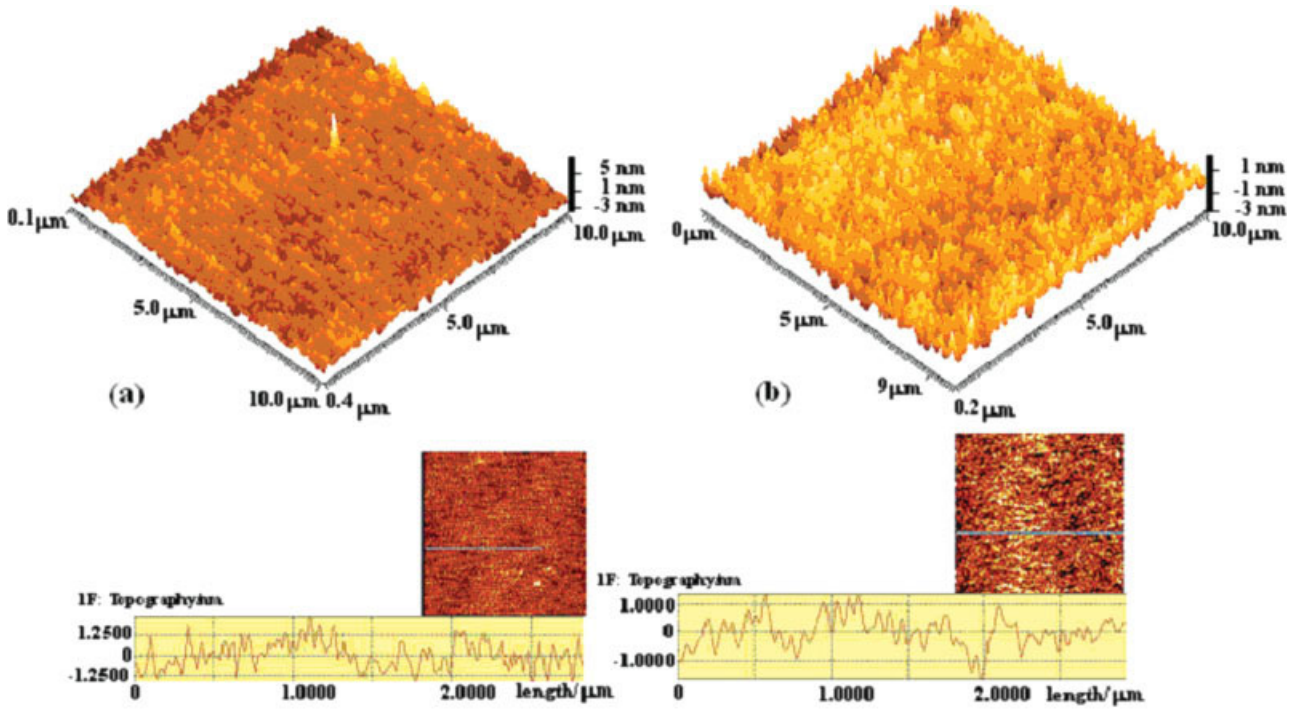

Figure 3. AFM images and corresponding cross sections of the film based on T-PAc2 (a) before and (b) after 110 min of UV exposure.

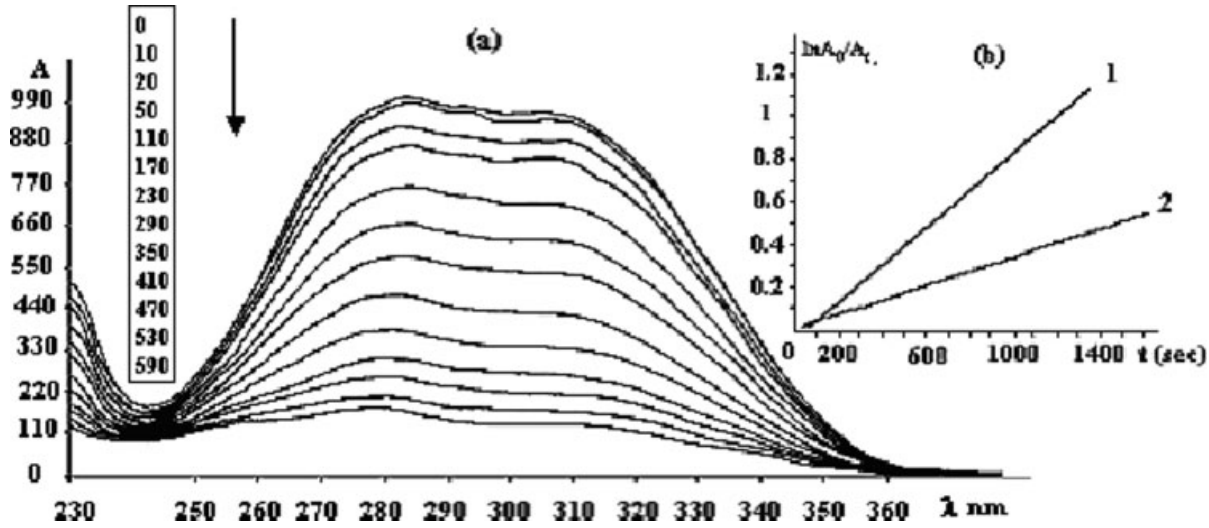

Figure 4. (a) Ultraviolet–visible spectral changes for P1 during UV irradiation and (b) dependence of the relative absorbance on the irradiation times (1) for P1 in methanol and (2) for T-PAc1 in a DMF solution.

morphology of compact particles distributed over the entire substrate without any tendency for agglomeration. Although T-PAc2 forms a good-quality film, its surface is not so flat and clean, and this results in numerous hills and valleys placed in a very smooth structure. The aspect ratio of the height and diameter has been confirmed by a cross section of 2 μm. This seems to provide direct evidence for the presence of relatively nanophase-separated domains that appear less distinct and have, on average, smaller lamellae or crystallites randomly disseminated throughout the surface of the film. The distribution of multichain aggregates of various sizes arranged in a quasilinear mode can be observed in the profilometric curve attached to this figure. Following then the image of the surface for the T-PAc2 film kept under UV irradiation for 110 min, when the triazene maximum completely disappeared in the UV spectrum (discussed later), we detected no obvious changes with AFM analysis [Fig. 3(b)]. At first glance, the absence of surface damage confirms that the photodecomposition of triazene chromophore caused by UV light does not affect the surface morphology.

Photobehavior of the Triazene Monomers and Copolymers

Because the triazene polymers are intended for applications in microlithography, it is important to study the photodecomposition of the triazene moiety both in the triazene precursors and in the derived copolymers. From this viewpoint, the photobehavior of P1 and P2 has been followed by the visualization of the change in the π–π^* transition of the triazene unit during irradiation with a high-pressure mercury lamp. The former absorbs in the UV spectrum at 284 and 308 nm, whereas P2 presents a single absorption band at 360 nm. Figure 4(a) shows UV absorption spectral changes for P1 in a methanol solution over various irradiation times. Under these conditions, there is a gradual decrease in both absorption maxima with the irradiation time. Exhaustive irradiation causes the disappearance of the earlier mentioned peak. Such a photoresponse, registered in about 9 min of irradiation, suggests an irreversible cleavage of the phenyl triazene chromophore in P1. Its kinetic evaluation [Fig. 4(b), plot 1] can be expressed by a first-order rate equation: $\ln(A_0/A_t) = kt$, where A_0 and A_t are the values of the absorbance at times t_0 and t, respectively, and k is a rate constant. Accordingly, the k value calculated for the phenyl triazene precursor is $k = 2.48 \times 10^{-3}$ s^{-1}. In comparison, for P2, in which the phototransformation degree is almost 30% after 144 min, $k = 4.9 \times 10^{-5}$ s^{-1} has been found. The lower photoreactivity in P2 is caused by the electron-withdrawing substituent of the triazene function.

To obtain further insight into the substituent effects, we have examined the structural changes of the triazene chromophore of each copolymer with absorption bands in UV spectra at 286 and 322 nm (T-PAc1) or 364 nm (T-PAc2) in DMF solutions. For a T-PAc1 solution, its photodecomposi-

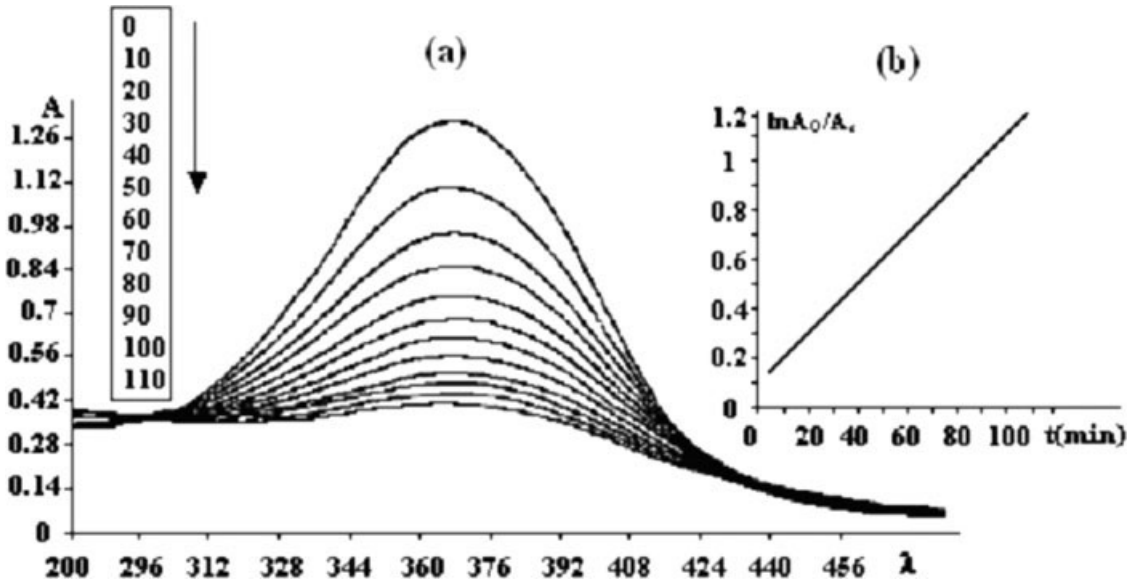

Figure 5. (a) Ultraviolet–visible spectral changes in a polymeric film (T-PAc2) upon UV irradiation and (b) its kinetics.

tion occurred within 30 min, whereas for the polymer with *p*-nitrophenyl triazene, a phototransformation of about 56% was attained after more than 200 min of exposure to UV light. A comparison of the kinetic plots indicates that this reaction took place faster for T-PAc1 ($k = 8 \times 10^{-3}$ s^{-1}) in a DMF solution [Fig. 4(b), plot 2] than for T-PAc2 ($k = 6.6 \times 10^{-5}$ s^{-1}). Moreover, for both polymers, the photoprocess follows first-order kinetics. Therefore, this result confirms again that the electron-acceptor substituent adjacent to the triazene function increases the stability of the polymers to UV photolysis. Similar data have been obtained for triazene diols used as partners in the synthesis of polyurethanes.[19]

Because the spectral changes induced by UV light in thin films are of practical interest, the rates of photolysis of the triazene polyacrylates have been determined under the same experimental conditions. An examination of the absorption maxima centered at 284 and 313 nm for T-PAc1 films has indicated that indeed the photodecomposition of the triazene function is induced almost completely in 15 min (ca. 95% transformation degree). Plotted in Figure 5(a,b) are the changes in the apparent percentage of phenyl triazene phototransformation in a T-PAc2 film. In comparison with T-PAc1, for which $k = 2.3 \times 10^{-3}$ s^{-1} has been calculated, the photodecomposition in the T-PAc2 film occurs more slowly ($k = 2 \times 10^{-4}$ s^{-1}). A possible decomposition scheme for triazene polyacrylates is shown in Scheme 3. In the first step of the photoprocess, we assume a trans–cis photoisomerization of the *N*=*N* bond with the formation of the cis isomer, which is thermodynamically more instable. Once formed, this isomer can photochemically be decomposed to aminyl macroradicals and phenyl or *para*-nitrophenyl diazenyl radicals. The diazenyl radicals are able to generate molecular nitrogen, leading to phenyl/*para*-nitrophenyl species that can be stabilized by hydrogen extraction or recombination. Similar photochemical reactions in the case of aminyl macroradicals are presumably responsible for the formation of crosslinked polyacrylates or polymers with pendant amino groups.

To probe the idea that the fragmentation of triazene groups via photolysis with UV light is accompanied by a crosslinking effect of the polymer, an experiment with a T-PAc1 film was performed. The film was irradiated for 2 h and then developed in $CHCl_3$. A decrease in the solubility for the irradiated area with increasing irradiation time suggests the irreversible decomposition of the triazene chromophore and photocrosslinking of the polymeric film.

Laser Ablation of the Triazene Acrylic Copolymers

The laser ablation rates at 308 nm versus the irradiation fluence are shown in Figure 6 for both triazene polyacrylates (T-PAc1 and T-PAc2), for which two distinct regions are notable. From the lower region, F_{th} can be determined, that is,

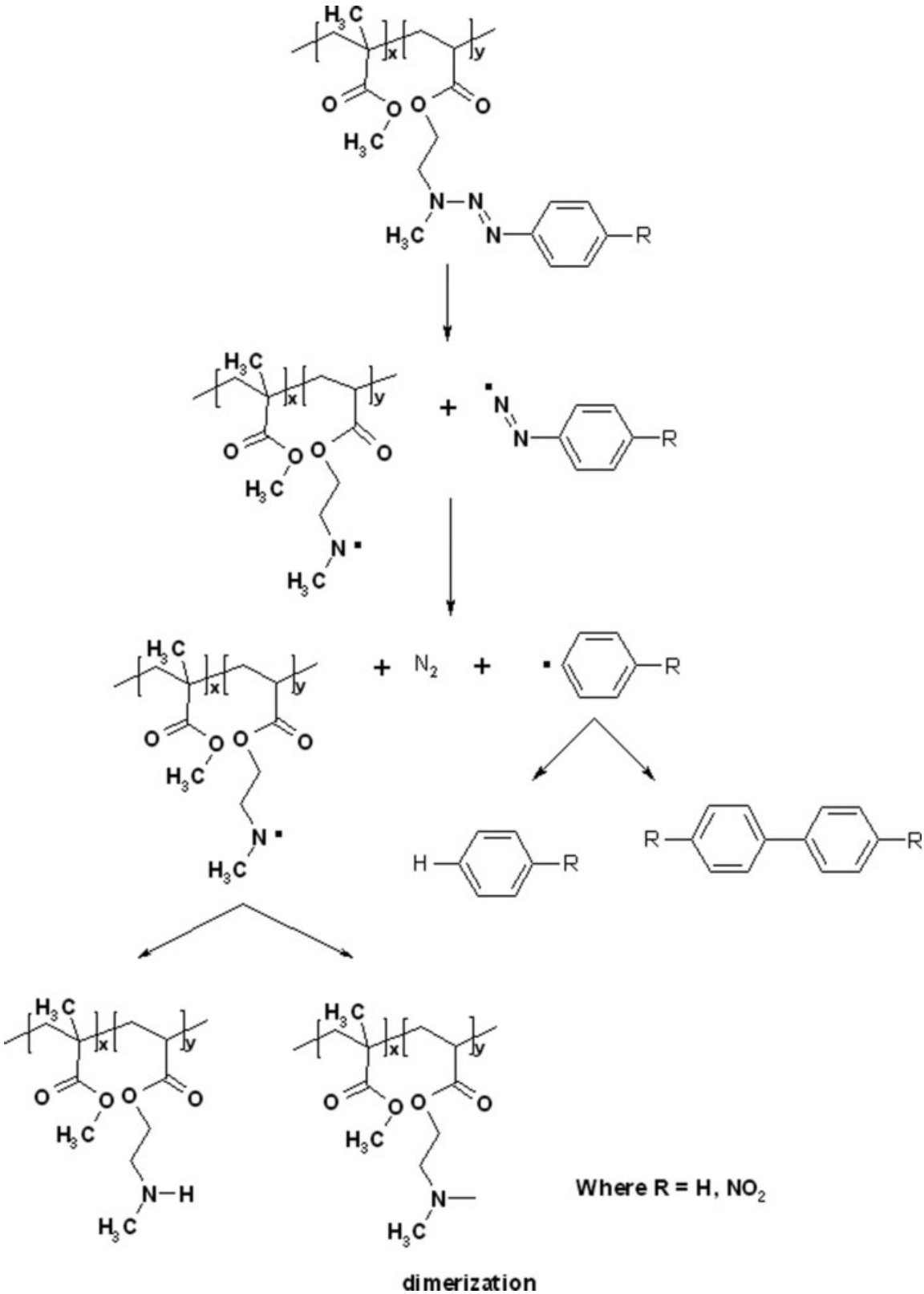

Scheme 3. Idealized representation of the photodecomposition of the triazene copolyacrylates.

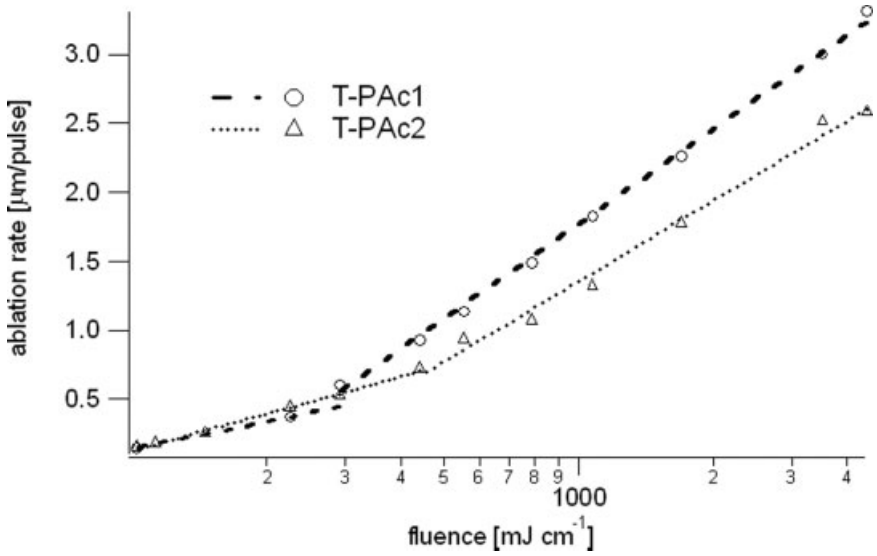

Figure 6. Ablation rate versus the fluence for T-PAc1 and T-PAc2 with irradiation at 308 nm.

60 mJ cm^{-2} for T-PAc1 and 70 mJ cm^{-2} for T-PAc2. The lower F_{th} value for T-PAc1 clearly indicates that the phenyl triazene is more sensitive to 308-nm irradiation than the nitrophenyl triazene group. This is consistent with studies performed on dialkyl phenyl triazenes, for which the nitro-substituted compounds are also less sensitive in comparison with nonsubstituted ones.[32] In tandem with the aforementioned, the higher α_{eff} values found in both regions for T-PAc1 (low fluence at 35,200 cm^{-1} and high fluence at 10,200 cm^{-1}) compared with those of T-PAc2 (low fluence at 11,200 cm^{-1} and high fluence at 5200 cm^{-1}) correspond to high ablation rates. In addition, the linear absorption coefficient at the irradiation wavelength is higher for T-PAc1 (52,300 cm^{-1}) than for T-PAc2 (31,700 cm^{-1}), suggesting a lower penetration depth of the laser photons. If the absorbed photons do not cause a bond breakage, they can induce fluorescence (not observable here) or heating via vibrational relaxation. Subsequently, additional heat could appear by the decomposition of triazene chromophores with effects on the increase in the polymer softening temperature. Taking into consideration that this temperature is 62 °C for PAc1 and 58 °C for PAc2, one would assume that the nitrophenyl triazene copolymer starts to flow (the round edges of the ablation spot, as observed for T-PAc2) when it is heated above the melting temperature but below the decomposition temperature. In comparison with T-PAc2, only partial melting on the edge has been observed for T-PAc1. Studies of PMMA confirm that this is a UV-softened polymer[33] that flows below its glass-transition temperature after UV irradiation. Some SEM photographs of our ablated films are shown in Figures 7 and 8, where one can see interesting effects of the exposure fluence on the physical conditions of the etched surface. After exposure, the T-PAc1 film shows a clear

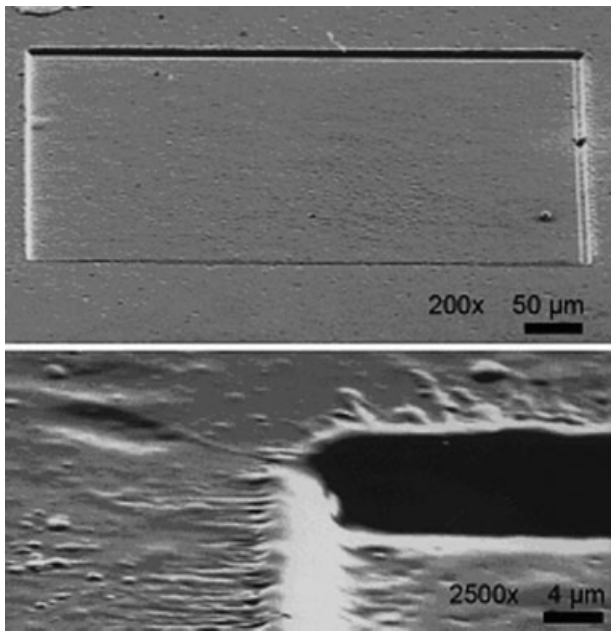

Figure 7. SEM images of T-PAc1 after 308-nm irradiation for five pulses at 550 mJ cm^{-2}. The whole ablation spot is shown in the top image; a close-up of the thermal features is shown in the bottom image.

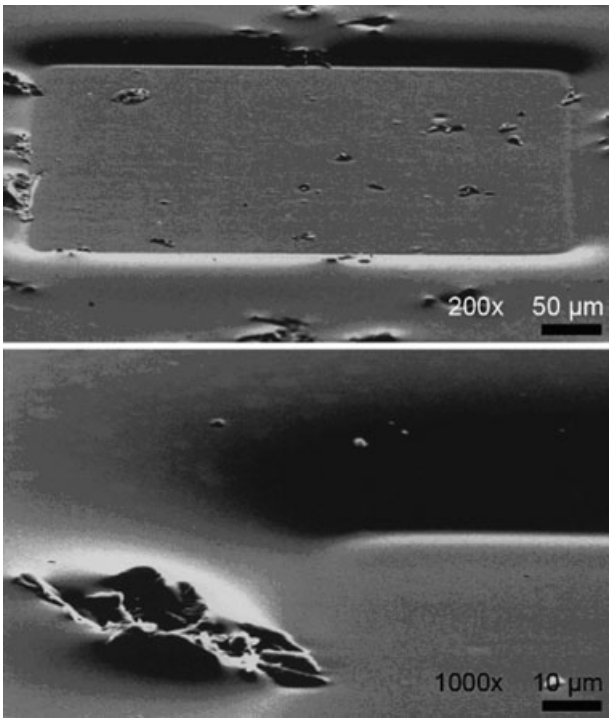

Figure 8. SEM images for T-PAc2 after 308-nm irradiation for five pulses at 3500 mJ cm^{-2}. The whole ablation spot is shown in the top image; a close-up of the flowing edges is shown in the bottom image.

ablation structure, in which the thermal features of the ablation mechanism are visible only with 2500× magnification (the lower image in Fig. 7). The rough structures of the films after drying are most likely caused by the presence of crystallites or small impurities in the polymer. However, the profile measurements clearly demonstrate that the phenyl triazene group is more suitable for laser structuring than the nitrophenyl triazene group, for which more pronounced thermal effects are observed, that is, flowing of the edges.

Details of the mechanism from a photophysical (thermal) viewpoint will be published elsewhere.

CONCLUSIONS

Two new triazene copolymers based on M1 or M2 and MMA were synthesized and characterized. The copolymers reported here had polymer compositions of 1:3.18 M1/MMA and 1:2.45 M2/MMA, respectively, as determined by NMR analysis. The photoreactivity of the triazene precursors and the resulting copolymers under Hg-lamp irradiation was dependent on the structure of the triazene chromophore. The phenyl triazene monomer led to copolymers with a higher photosensitivity to UV irradiation than those with nitrophenyl triazene. The irradiation of the polymer films up to the complete disappearance of the characteristic peak for the triazene group in the UV spectrum had no effects on the surface morphology viewed in the AFM image. This result supports the idea that the photodecomposition of the triazene chromophore, which occurs by first-order kinetics, does not induce surface damage. This ablation work clearly demonstrates that the ablation of triazene copolymer films can be caused by laser exposure at 308 nm even with a higher ablation rate for the phenyl triazene copolymer.

The authors thank the Ministry of Research and Education for its financial support of this work through the National Research Programme (MEC CNCSIS; project no. 32952/2004).

REFERENCES AND NOTES

1. Natansohn, A.; Rochon, P. Chem Rev 2002, 102, 4139.
2. Gupta, P.; Trenor, S. R.; Long, T. E.; Wilkes, G. L. Macromolecules 2004, 37, 9211.
3. Morigaki, K.; Schönherr, H.; Frank, C. W.; Knoll, W. Langmuir 2003, 19, 6994.
4. Nuyken, O.; Scherer, C.; Baindl, A.; Brenner, A.; Dahn, U.; Gartner, R.; Kaiser-Rohrich, S.; Kollefrath, R.; Matusche, P.; Voit, B. Prog Polym Sci 1997, 22, 93.
5. Lippert, T.; Hauer, M.; Phipps, C.; Wokaun, A. Proc SPIE-Int Soc Opt Eng 2002, 4760.
6. Lippert, T.; David, C.; Hauer, M.; Wokaun, A.; Robert, J.; Nuyken, O.; Phipps, C. R. J Photochem Photobiol A 2001, 145, 87.
7. Lippert, T.; Hauer, M.; Phipps, C. R.; Wokaun, A. Appl Phys A 2003, 77, 259.
8. Wei, J.; Hoogen, N.; Lippert, T.; Nuyken, O.; Wokaun, A. J Phys Chem B 2001, 105, 1267.
9. Stebani, J.; Nuyken, O.; Lippert, T.; Wokaun, A. Makromol Chem Rapid Commun 1993, 14, 365.
10. Furutani, H.; Fukumura, H.; Masuhara, H.; Lippert, T.; Yabe, A. J Phys Chem A 1997, 101, 5742.
11. Lippert, T.; Dickinson, J. T. Chem Rev 2003, 103, 453.
12. Hahn, C.; Kunz, T.; Dahn, U.; Nuyken, O.; Wokaun, A. Appl Surf Sci 1998, 127, 899.
13. Hoogen, N.; Nuyken, O. J Polym Sci Part A: Polym Chem 2000, 38, 1903.
14. Lau, A. N. K.; Vo, L. P.; Fone, M. M.; Duff, D. W.; Merlino, G. J Polym Sci Part A: Polym Chem 1994, 32, 1507.

15. Lippert, T.; Wokaun, A.; Stebani, J.; Nuyken, O.; Ihlemann, J. Angew Makromol Chem 1993, 206, 97.
16. Nuyken, O.; Dahn, U.; Ehrfeld, W.; Hessel, V.; Hesch, K.; Landsiedel, J.; Diebel, J. Chem Mater 1997, 9, 485.
17. Stebani, J.; Nuyken, O.; Lippert, T.; Wokaun, A. Makromol Chem Rapid Commun 1993, 14, 365.
18. Hauer, M.; Lippert, T.; Wokaun, A. Appl Phys A 2004, 79, 1215.
19. Buruiana, E. C.; Melinte, V.; Buruiana, T.; Lippert, T.; Yoshikawa, H.; Mashuhara, H. J Photochem Photobiol A 2005, 171, 261.
20. Buruiana, E. C.; Melinte, V.; Buruiana, T.; Simionescu, B. C. J Appl Polym Sci 2005, 96, 385.
21. Buruiana, E. C.; Melinte, V.; Buruiana, T. J Appl Polym Sci 2004, 92, 2599.
22. Buruiana, E. C.; Melinte, V.; Buruiana, T. J Appl Polym Sci 2003, 88, 1203.
23. Buruiana, E. C.; Buruiana, T.; Strat, G.; Strat, M. J Photochem Photobiol A 2004, 162, 23.
24. Buruiana, E. C.; Buruiana, T.; Strat, G.; Strat, M. J Polym Sci Part A: Polym Chem 2002, 11, 1918.
25. Buruiana, E. C.; Buruiana, T.; Strat, G.; Strat, M. J Polym Sci Part A: Polym Chem 2005, 43, 3945.
26. Buruiana, E. C.; Olaru, M.; Strat, M.; Strat, G.; Simionescu, B. C. Polym Int 2005, 54, 1296.
27. Buruiana, T.; Buruiana, E. C. J Polym Sci Part A: Polym Chem 2004, 42, 5463.
28. Buruiana, E. C.; Buruiana, T. J Photochem Photobiol A 2002, 151, 237.
29. Buruiana, T.; Buruiana, E. C. J Appl Polym Sci 2002, 86, 1240.
30. Buruiana, E. C.; Buruiana, T. Polym J 2001, 33, 723.
31. Andrew, J. E.; Dyer, P. E.; Forster, D.; Key, P. H. Appl Phys Lett 1983, 43, 717.
32. Srinivasan, R.; Braren, B. J Polym Sci Part A: Polym Chem 1984, 22, 2601.
33. Masuhara, H.; Hiraoka, H.; Domen, K. Macromolecules 1987, 20, 450.